PASSIVE MEASUREMENT OF DUST PARTICLES ON THE ISS USING MPAC: EXPERIMENT SUMMARY, PARTICLE FLUXES AND CHEMICAL ANALYSIS

Michael J. Neish[(1)], Yukihito Kitazawa[(2)], Takaaki Noguchi[(3)], Toshihiko Inoue[(1)], Kichiro Imagawa[(1)], Tateo Goka[(1)], Yoshiyuki Ochi[(4)]

[(1)] Japan Aerospace Exploration Agency, 2-1-1 Sengen, Tsukuba City, Ibaraki Pref. 305-8505, Japan.
E-mail mike@jaxa.jp, inoue.toshihiko@jaxa.jp, imagawa.kichiro@jaxa.jp
[(2)] Ishikawajima-Harima Heavy Industries Co. Ltd., Shin-Ohtemachi Bldg., 2-2-1, Ohtemachi, Chiyoda-Ku, Tokyo 100-8182, Japan.
E-mail: yukihito_kitazawa@ihi.co.jp
[(3)]Department of Materials and Biological Sciences, Ibaraki University, 2-1-1 Bunkyo, Mito, Ibaraki Pref. 310-8512, Japan.
[(4)] Advanced Engineering Services Co. Ltd, 1-6-1 Takezono, Tsukuba City, Ibaraki Pref. 305-0032, Japan.
E-mail: ochi.yoshiyuki@jaxa.jp

ABSTRACT

MPAC&SEED is a JAXA-owned experiment for particle capture and material exposure mounted on an aluminium tray that can be folded into a suitcase for transportation. Three such trays have been placed on the exterior of the Russian Service Module (SM) of the International Space Station (ISS). Two have already been retrieved.

We describe the overall experiment, and provide details and results of the post-flight inspection and analysis so far obtained, including some chemical data. In addition, we provide details of extensive contamination observed on the surfaces of the experiment, particularly in aerogel, that we believe is worth considering when designing future experiments of this type that utilise the ISS.

1. INTRODUCTION

The Micro-Particles Capturer (MPAC) is a passive experiment designed to sample the micrometeoroid and space debris environment, and capture particle residues for later chemical analysis. It is mounted on a collapsible frame, about 1 m long when open, which it shares with the Space Environment Exposure Device (SEED), a materials exposure experiment.

Three identical MPAC&SEED units were launched aboard Progress M-45 on 21 August, 2001, and attached side-by-side to a handrail outside the SM by extra-vehicular activity (EVA) on 15 October, 2001. The first unit (hereafter MPAC #1) was retrieved on 26 August, 2002, after 315 days' exposure, and returned to Earth shortly afterwards. MPAC #2 was retrieved on 26 February, 2004 after 864 days' exposure. Fig. 1 is a photograph of MPAC&SEED in flight, with trays #1 and #2 indicated.

MPAC consists of three materials: aerogel and polyimide foam for particle capture, and a 6061-T6 aluminium witness plate to provide simple crater counts. The number of tiles and exposed areas of each tile are summarised in Table 1 for each material. Fig. 2 is a photograph of the ram and wake faces of one MPAC&SEED tray.

The densities of aerogel and polyimide foam used are 0.03 g cm^{-3} and 0.011 g cm^{-3} respectively. When micrometeoroids or small space debris particles strike these materials, they decelerate gradually with reduced shock pressures and temperatures; thus there is a better chance of recovering significant residues for chemical analysis.

As polyimide foam is susceptible to atomic oxygen (AO) attack, exposed surfaces of this material on both the ram and wake have been covered with a 12.5-µm-thick polyimide film (UPILEX-R™), fortified with a vapour-deposited gold coating, which provides strong, if not complete, AO-resistance. The films are not fixed

Table 1. Exposed surface areas of one tile of each of the three MPAC materials, including thickness.

	Ram Face		Wake Face	
Material	**Tiles**	**Exposed Area of *One* Tile/Plate**	**Tiles**	**Exposed Area of *One* Tile/Plate**
Aerogel	24	3.7 x 3.7 cm (thickness 1.55 cm)	24	3.7 x 3.7 cm (thickness 1.55 cm)
Polyimide Foam	2	each tile exposed in two windows: 5.0 x 7.85 cm* (thickness 3 cm) each tile exposed in two windows: 5.0 x 6.3 cm (thickness 0.7 cm)	1	tile exposed in two windows: 5.0 x 7.85 cm (thickness 3 cm)*
6061-T6 Aluminium Plate	1	13.6 x 15.25 cm (thickness 0.2 cm)	–	–

*the same tile has both ram- and wake-exposed surfaces.

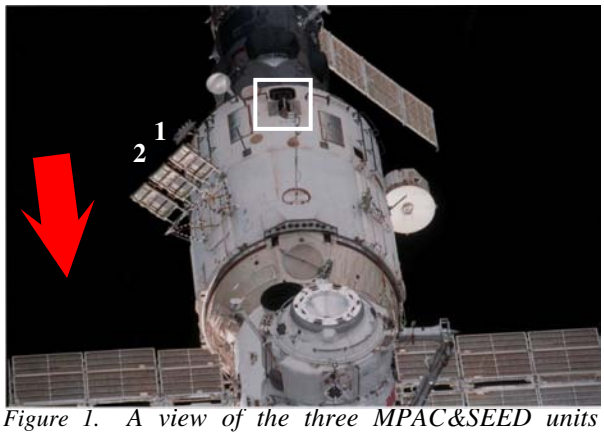

Figure 1. A view of the three MPAC&SEED units during exposure. The velocity vector (in the XVV flight mode) points approximately along the ISS long axis as indicated by the arrow, while the ISS-Earth vector lies perpendicular to it, pointing approximately upwards as seen in the image. The two retrieved units, 1 and 2, are indicated (image courtesy of The Boeing Company).

to the foam underneath, but are held in position by a frame that is screwed down over the foam. Removing the frame therefore releases the films. Aerogel needs no protection, since it is unaffected by AO.

It is also to be noted that the ram- and wake-exposed surfaces of the polyimide foam are actually the opposite faces of the same tiles.

Although the front and back faces of MPAC&SEED are termed "ram" and "wake" faces respectively, in fact they were truly so only for about 60% of the total exposure period of MPAC #1, when the ISS was in XVV flight mode (X-axis along the Velocity Vector). For the remaining 40% of the time, approximately, the ISS was in XPOP flight mode (X-axis Perpendicular to the Orbital Plane), whereby the ISS long-axis, and therefore the ram face of MPAC&SEED, pointed along the orbital angular momentum vector (orbital north). Moreover, the orientation of the ISS typically deviated from true XVV and XPOP by several degrees. However, for the sake of simplicity, we will retain the above naming convention. Later, regular YVV (Y-axis along the Velocity Vector) was introduced, in which MPAC&SEED was also nominally oriented north-south, and so the exposure conditions as far as micrometeoroid and debris flux is concerned, are identical except for the small shielding factor due to the ISS body, and the particular yaw, pitch and roll angles of the ISS at the time.

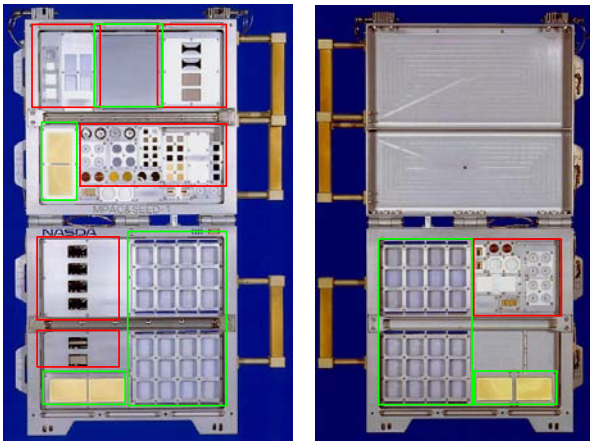

Ram face **Wake face**

Figure 2. One MPAC&SEED tray.

After MPAC #1 and #2 were retrieved and transported to Japan, close visual examinations were conducted during which all major features of interest on the test materials and experimental frame were photographed and documented, including evidence of contamination, discoloration and other damage to the materials.

The small area-time product of the experiment requires that small-sized features be located, in order to obtain meaningful statistics. Just how small can be estimated with the use of micrometeoroid and debris models: we have used MASTER-2001 (Krag *et al.*, 2002). The number of tiles or plates of each material, their total

Table 2. Total exposed surface area of each of the three MPAC materials, on the Ram and Wake faces, and expected hits by particles greater than or equal to three different particle diameter limits, d. The left-hand value in each cell is for MPAC #1, and the right-hand one for MPAC #2.

Ram Face					
Material	**Tiles or Plates**	**Surface Area [cm^2]**	**Expected Hits [$d \geq 5$ µm]**	**Expected Hits [$d \geq 10$ µm]**	**Expected Hits [$d \geq 15$ µm]**
Aerogel	24	328.6	22.2 / 60.8	9.9 / 27.2	6.2 / 17.0
Polyimide Foam	2	141.5	9.6 / 26.2	4.2 / 11.5	2.7 / 7.4
6061-T6 Al Plate	1	207.4	14.0 / 38.4	6.2 / 17.0	3.9 / 10.7

Wake Face					
Material	**Tiles or Plates**	**Surface Area [cm^2]**	**Expected Hits [$d \geq 5$ µm]**	**Expected Hits [$d \geq 10$ µm]**	**Expected Hits [$d \geq 15$ µm]**
Aerogel	24	328.6	16.6 / 45.5	7.5 / 20.6	4.5 / 12.3
Polyimide Foam	1	78.5	4.0 / 11.0	1.8 / 4.9	1.1 / 3.0

exposure area and the expected number of hits by particles of diameter $\geq d$ for d = 5, 10 and 15 µm are summarised in Table 2 for the ram and wake faces of MPAC #1 and #2, assuming 60% true ram-wake exposure, and 40% true north-south exposure (i.e., XPOP or YVV mode) for the entire 315-day and 864-day periods. These are *unshielded* fluxes – the shielding factor is estimated to be about 15-20% for micrometeoroids – which are estimated to outnumber space debris particles at these sizes by up to a factor of 20-40, according to MASTER-2001. Detailed directional analysis is required for a more accurate estimate.

The next section summarises what has been achieved so far by way of post-flight analysis.

2. INSPECTION BY MATERIAL

2.1 Polyimide Foam

The cover films were scanned while still in the experimental frame, since removing the tiles would have resulted in separation of film and foam. Scanning was done using a special colour CCD attachment to a laser microscope, at a magnification of 350x, at which 20-µm impacts were easily distinguishable from other features, but anything smaller than 15 µm required some judgement. Table 3 summarises the total number of impacts found on MPAC #1 and #2 Ram and Wake film.

Table 3. Total number of impacts found in MPAC #1 and #2 cover film.

	Ram	Wake
MPAC #1	20	0
MPAC #2	26	6

After recording all the impacts, pin-holes were inserted at a number of points in each film, through into the underlying foam, to fix the coordinates of both materials to each other, and enable the entry holes in the foam to be located.

The frame holding down the film was then removed, releasing the film. Additional images were then able to be taken of the impact features using a laser microscope and optical CCD zoom lens. These were also photographed from the rear side.

Inspecting the underlying foams for impact holes has been a disappointment, since none could be identified in either of the MPAC #1 foams. In MPAC #2 only one entry hole has been located, that of the largest impact found so far in this material, shown in Fig. 3 (left). This is a highly-elongated, irregular impact with an unusual morphology. In the foam surface (right) there is an obvious burn mark surrounding the foam entry hole, which extends deep into it, but does not reach the back face. The arrow indicates the impact direction, which was evidently almost grazing. The reason for generally not being able to locate the entry holes in the foam is that the natural pores in the foam were larger than the impacting particles.

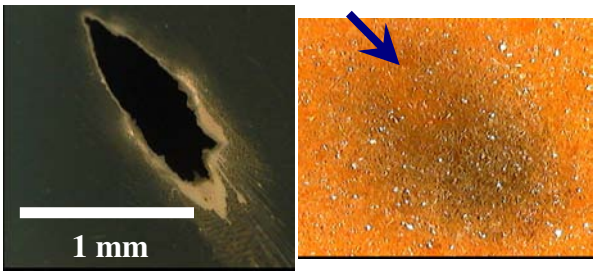

Figure 3. Largest impact found in polyimide film, and the only one leaving a discernible impact hole in the underlying foam. The impact direction is shown by the arrow. Images are not to scale.

Fig. 4 (top) shows two typical perforations found in the cover film. Fig. 4 (bottom) shows two examples of several features found in the films that appear to be impacts of some description, but have a very different morphology from that of classic thin-film perforations.

None of these features appears to be a complete perforation, despite having diameters far in excess of the film thickness. All are elongated, and concentric marks surround the central feature. Their shallow depth points to the possibility that they are low-velocity impacts, even particulate contamination from the ISS itself, but this remains to be confirmed.

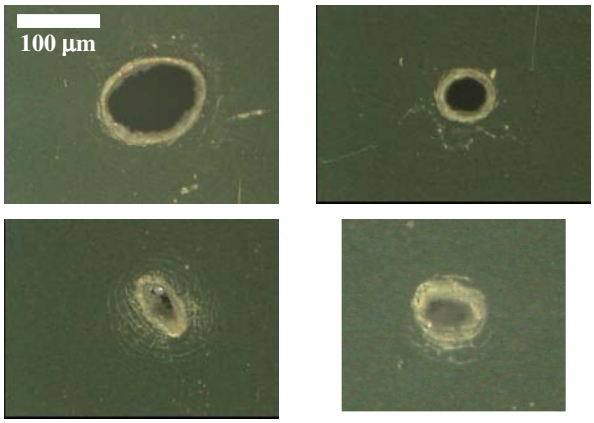

Figure 4. (top) Two typical perforations in the cover film; (bottom) two impacts with unusual morphology. Images to scale.

Fig. 5 shows the film fluxes for the ram faces of both MPACs #1 and #2 (thin lines with error bars) plotted in terms of particle flux (m^{-2} yr^{-1}) as a function of hole diameter in the cover film, D_h (in the case of perforations), or crater diameter, D_c, (in the case of non-perforations), both measured at the surface intercept. For comparison, the MASTER-2001 model

fluxes for micrometeoroids and space debris are also shown.

As MASTER-2001 calculates fluxes as a function of particle diameter, d, this has to be converted to D_h. No relationship between the two parameters has been derived for Upilex; however Neish *et al.* (2001) derived one for Kapton using electrothermal gun data. On the premise that Upilex and Kapton will be very similar – not unreasonable given that Neish *et al.* (2001) also showed that Kapton and Teflon have similar response curves – the Kapton equation is used here, which is:

$$\frac{d_p}{T} = A\frac{D_h}{T}V^B, \qquad (1)$$

[valid range: $V = 4 – 9$ km s^{-1}; $D_h/T = 0.5 – 4$]

where A and B are empirically-determined parameters equal to 4.09371 and -1.0671, V is the normal impact velocity, and T the film thickness. Thus a fit through the data points within the stated velocity range and hole size is an almost linear relationship in V between d_p and D_h. Analysis using MASTER-2001 gives a mean normal impact velocity on MPAC of about 13.5 and 10.7 km sec^{-1} on the ram and wake face respectively, which is outside the valid range of equation (1). Applying the equation would give a D_h/T ratio on the ram face of about 3.9. Intuitively, this could be an overestimate (a linear relationship between D_h and d_p is not likely to extend indefinitely). Until more experimental data are available, the D_h/d_p ratio will be assumed to be between 3.9 and the value obtained at the upper limit of the valid velocity range (9 km s^{-1}), which gives a value of 2.55. Thus, there are two curves for the MASTER-2001 model in Fig. 5, for d_p converted using both factors. The "true" curve is considered to lie somewhere in between.

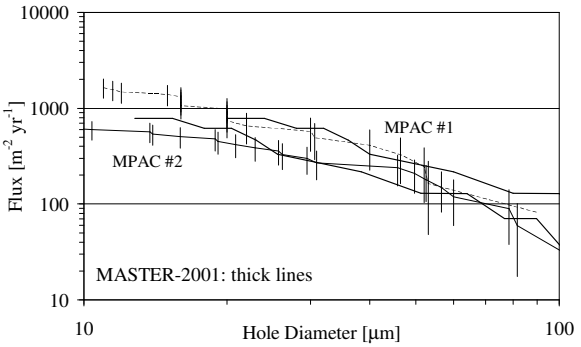

Figure 5. Flux [m^{-2} yr^{-1}] calculated from the polyimide film impacts, compared to the MASTER-2001 model fluxes for micrometeoroids and space debris.

2.2 Silica aerogel

The aerogel tiles also underwent an initial, quick naked-eye inspection soon after transportation of the experimental frames to JAXA. Each tile was then removed and stored in its own container.

Scanning for impact features was done using an optical CCD zoom lens at a magnification of 150x. Where necessary, a fibre-optic light source was used to enhance contrast by means of side-lighting.

Scanning of MPAC #1 aerogel was aimed at locating features 50 μm in size, along the largest dimension, or greater. However, this limit had to be increased to 100 μm in MPAC #2 aerogel in view of serious surface alterations in the material, due to contamination (Section 4). The entry hole and track were photographed in each case. Owing to the transparency of aerogel, it was also possible to photograph impacts tracks at different points along their depth and combine them into a mosaic.

Track length and depth were measured, enabling track angle with respect to the surface to be calculated. Track ends were given special attention in case the presence of residues could be ascertained. Track lengths and angles in MPAC #1 are discussed by Kitazawa *et al.* (2004a and 2004b)

Interesting features were then sectioned by cutting a slice oriented in the direction of the impact track with a razor, so that it could be viewed and photographed from the side. A number of features have so far been selected for chemical analysis (section 3).

One more objective of the aerogel inspection is to assess the morphology of the aerogel features according to criteria set out by Kitazawa *et al.* (1999).

2.3 6061-T6 Aluminium Plate

The aluminium plates were scanned at a magnification of 375x. Only four impacts were located in the MPAC #1 plate, and six in that of MPAC #2, yields that appear low when compared with estimates in Table 2. Because of pock-marks and other imperfections in the aluminium it is possible that some of the smaller craters may have been overlooked. The diameters of the four features found in the MPAC #1 plate are 29, 25, 24 and 24 μm. Those of the six features found in the MPAC #2 plate are 104, 74, 33, 30, 19 and 15 μm. For space considerations, and because the number of craters is too small for meaningful flux curves, further discussion of this data is omitted.

3. CHEMICAL ANALYSIS

Chemical analysis of aerogel is being conducted at Ibaraki University. So far, a number of interesting features have been selected for analysis: either large tracks or those displaying classic morphology.

Chemical analysis of MPAC #1 features was done *in situ*, i.e., the block of aerogel containing the impact track was placed in a scanning electron microscope, and residues analysed without any attempt to extract them. For MPAC #2 residues will be extracted wherever possible. Results from selected features now follows.

3.1 MPAC #1, Impact 3RC3

The largest feature found in MPAC #1 aerogel, on the ram side, is shown in Fig. 6 together with the result of EDX analysis performed on the inner wall of the impact track, as highlighted by the white oval. Aluminium was identified, which Raman spectroscopy subsequently indicated was in the pure form (as opposed to an oxide). This suggests a debris impact.

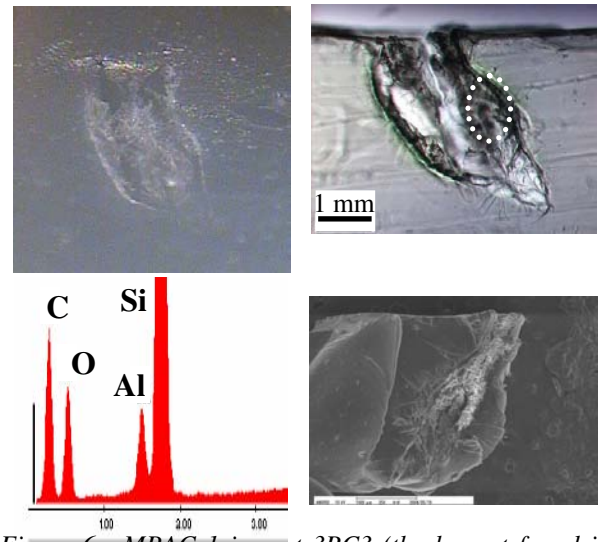

Figure 6. MPAC 1 impact 3RC3 (the largest found in MPAC1 aerogel: entry hold diameter ~2 mm, track length ~5 mm). The inner wall was subjected to EDX analysis, revealing Al. Si and O are constituents of aerogel, and C was used as a coating.

3.2 MPAC #2, Impact 4WD1

This large, typical carrot-shaped track (Fig. 7), over 1 mm long and almost perpendicular to the surface, revealed two possible impact residues, one just beyond the point after the track narrows, and one at the end. EDX analysis was conducted on both. The first one revealed Ag, Al and S, and could be orbital debris. The second revealed only background elements, and is thought to be altered aerogel.

3.3 MPAC #1, Impact 3RD3 #2

A grain about 20 µm in diameter was detected in this track. Its Raman spectrum matches that of rutile titanium dioxide, TiO_2 (*University of Parma mineral Raman spectra database*: see references), as shown in Fig. 8. Thermal control paint is known to contain this compound (Meshishnek, 1995); it is also found in some meteorites, but the absence of other elements and compounds points to the former as the source.

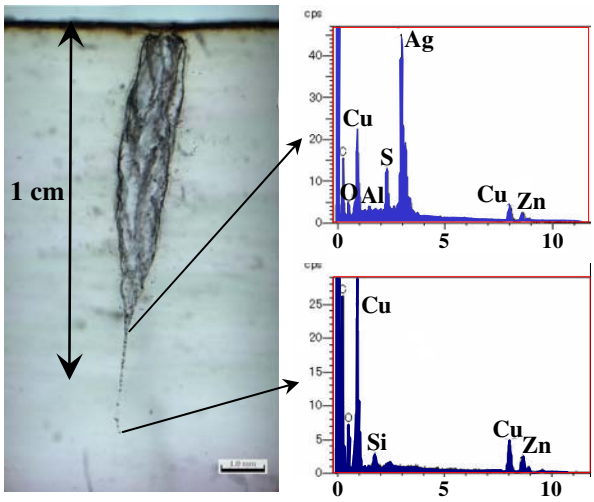

Figure 7. A typical carrot-shaped MPAC 2 impact. The first fragment revealed Ag, Al and S, the second background elements only.

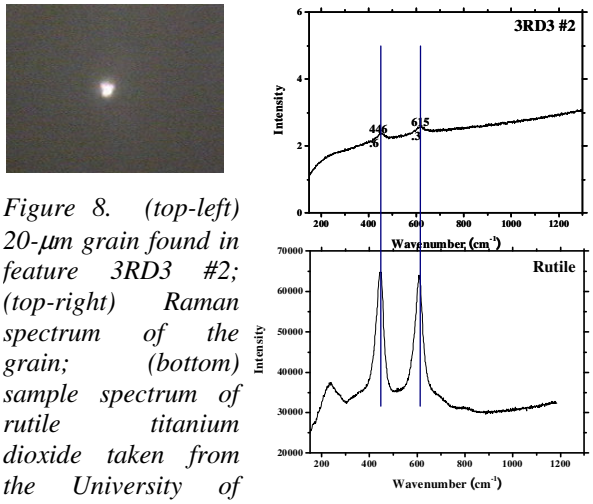

Figure 8. (top-left) 20-µm grain found in feature 3RD3 #2; (top-right) Raman spectrum of the grain; (bottom) sample spectrum of rutile titanium dioxide taken from the University of Parma Web page.

4. SURFACE ALTERATIONS

Considerable surface alterations have been observed in aerogel. Fig. 9 compares pristine aerogel with examples of the ram and wake surfaces in MPACs #1 and #2, to the same scale.

On the wake face, a brittle-looking crust has formed, undulating in places, with a texture resembling that of parched terrain, in some places like tree-rings. The texture is the same in MPACs #1 and #2, although the individual "cells" are smaller in size in the latter. This phenomenon has not been observed in earlier aerogel experiments, such as ODC (Hörz *et al.* 1999, 2000).

This effect has already adversely affected the post-flight analysis of MPAC #2 in that the minimum size threshold of impact features searched for in aerogel has had to be raised from 50 to 100 μm.

The ram-facing surfaces of MPAC #1 have become roughened with a number of pock-marks scattered over the tile. This effect is much more pronounced in MPAC #2, with the density of pock-marks totalling up to 4,000 per tile in places. Under the microscope they appear as holes of the order of 100-200 μm across, and have been branded "jellyfish" features by Kitazawa et al. (2004b)..

It is evident to the naked eye that the wake side of the experimental trays is generally covered in a uniform brown sheen of deposited contamination, not seen on the ram face. This effect is thought to be due to deposition from the nadir roll thrusters of the Russian Service Module, which are located in the wake of MPAC&SEED location during flight, highlighted by a rectangle in Fig. 1. Chemical analysis of contamination features show traces of Fe, N and Zn among other elements, which support this view.

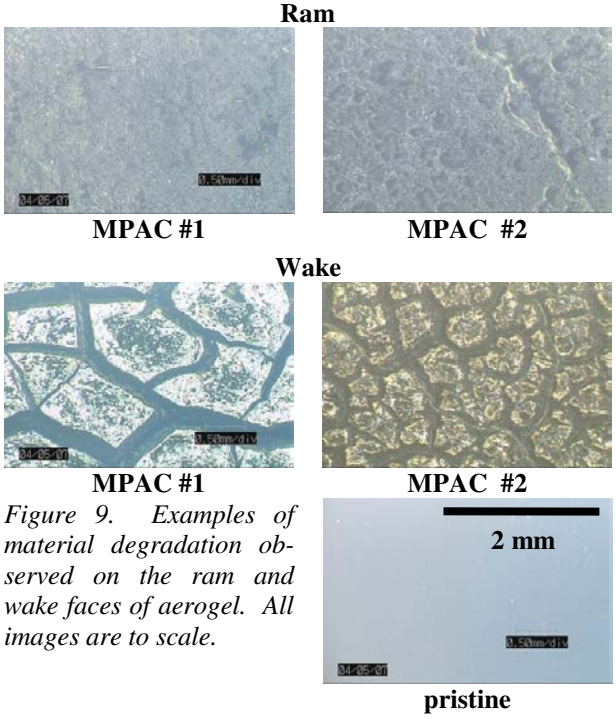

Figure 9. Examples of material degradation observed on the ram and wake faces of aerogel. All images are to scale.

5. CLOSING COMMENTS

The flux curves derived from the polyimide films appear to be broadly compatible with that of MASTER-2001, with particle diameter d_p converted to hole diameter D_h using an expression derived by Neish *et al*. (2001) from impact experiments into Kapton film.

Selected results of chemical analysis have been described here. An archive will be built up as the analysis progresses.

Data on track length and angle in MPAC #1 aerogel are described by Kitazawa *el al*. (2004a and 2004b). Inspection of MPAC #2 aerogel is progressing.

MPAC&SEED #3 is scheduled for retrieval in October 2005, after four years' exposure.

6. REFERENCES

Hörz, F., Cress, G., Zolensky, M., See, T. H., Bernhard, R. P. and Warren, J. L. (1999). "Optical Analysis of Impact Features in Aerogel from the Orbital Debris Collection Experiment on the MIR Station", *NASA Technical Memorandum TM-1999-209372*, available from http://setas-www.larc.nasa.gov/meep/meep.html.

Hörz F., Zolensky, M. Bernhard, R. P., See, T. H. and Warren, J. L. (2000). "Impact Features and Projectile Residues in Aerogel Exposed on Mir", *Icarus*, Vol. 147, 559-579.

Kitazawa, Y., Fujiwara, A., Kadono, T., Imagawa K., Okada, Y. and Uematsu, K., Hypervelocity Impact Experiments on Aerogel Dust Collector*, J. Geophys, Res*., Vol. 104, No. E9, 1999.

Kitazawa, Y., Noguchi, T., Neish, M.J., Inoue, T., Ishizawa, J., Fujiwara, A., Imagawa, K, Yamaura, Y., Watanabe, Y, Murakami, A. "First Year Mission Results of Passive Measurement Experiment of Dust Particles on ISS (MPAC)", to be published in *Proc of 24th Int. Symp. on Space Technology and Science*, Miyazaki, Japan, 30 May to 6 June 2004a.

Kitazawa, Y, Neish, M.J., Inoue, T, Imagawa, K, Fujiwara, A. "First Year Mission Results of Passive Measurement Experiment of Dust Particles on ISS (MPAC)", presented at the 35th COSPAR Assembly, Paris, France, 17-25 July 2004, to be published in *Adv. Sp. Res*., 2004b.

Krag, H., Bendisch, J., Bunte, K.D., Klinkrad H., Martin, C., Sdunnus, H., Walker, R., Wegener P. Wiedemann, C. Introducing the ESA-MASTER 2001 Space Debris Model. *Adv. Astron. Sciences*, Vol 112, Part II, "Spaceflight Mechanics", 2002.

Meshishnek, M.J. (1995). "Overview of the Space Debris Environment", *SMC-TR-95-9 Aerospace Report No. TR-95(5231)-3*.

University of Parma mineral Raman spectra database, http://www.fis.unipr.it./~bersani/raman/raman/spettri.htm